gemeinen aber auch nicht exakt Null sein, da der Faktor bei cos α zwar als Summe kleiner Glieder mit wechselnden Vorzeichen nahezu, aber nicht exakt Null ist. Durch das LS-Verfahren wird also die Koinzidenz von HTK^{g} und HTK^{frei}, $\alpha=0$, weitgehend realisiert. Somit wird das Verfahren von Milledge, in dem die Koinzidenz gesetzt wird, vom LS-Verfahren her bestätigt. Allerdings sollte man bei Atomen von verschiedener Grösse für ihre 'Masse' Z_i^2 ansetzen (oder auch σ_i^{-2}, angegeben in Å^{-2}-Einheiten, nicht aber σ_i^{-1}). Die 'Masse' entspricht also – in der angegebenen Näherung – gerade der Intensität der von dem betreffenden Atom ausgehenden Sekundärstrahlung.

Literatur

Buerger, M. J. (1960). *Crystal-Structure Analysis*, S. 585. New York, London.

Busing, W. R. & Levy, H. A. (1961). *Computing Methods and the Phase Problem in X-Ray Crystal Analysis*, S. 146. Oxford, London, New York, Paris.

Cochran, W. (1948). *Acta Cryst.* **1**, 138.

Cruickshank, D. W. J. (1959). *International Tables for X-ray Crystallography*, Vol. II, S. 330. Birmingham: Kynoch Press.

Diamond, R. (1964). Cambridge, England. Private Mitteilung.

Farag, M. S. (1954). *Acta Cryst.* **7**, 117.

Hughes, E. W. (1941). *J. Amer. Chem. Soc.* **63**, 1737.

Linnik, J. W. (1961). *Methode der kleinsten Quadrate in moderner Darstellung*. Berlin.

Milledge, H. J. (1962). *Proc. Roy. Soc.* A, **267**, 566.

Qurashi, M. M. (1953). *Acta Cryst.* **6**, 577.

Scheringer, C. (1963). *Acta Cryst.* **16**, 546.

Scheringer, C. (1965). *Acta Cryst.* **19**, 504.

Sparks, R. A. (1961). *Computing Methods and the Phase Problem in X-Ray Crystal Analysis*, S. 170. Oxford, London, New York, Paris.

Waser, J. (1963). *Acta Cryst.* **16**, 1091.

Watson, H. C. (1963*a*). Cambridge, England. Private Mitteilung.

Watson, H. C. (1963*b*). *Acta Cryst.* **16**, A185.

Zurmühl, R. (1964). *Matrizen und ihre technischen Anwendungen*, S. 202 und 212. Berlin, Göttingen, Heidelberg.

Acta Cryst. (1965). **19**, 524

Determination of the Crystal Structure of Yttrium Orthoferrite and Refinement of Gadolinium Orthoferrite*†

By P. Coppens

Department of X-ray Crystallography, The Weizmann Institute of Science, Rehovoth, Israel

and M. Eibschütz

Department of Electronics, The Weizmann Institute of Science, Rehovoth, Israel

(*Received* 29 *December* 1964)

The crystal structure of yttrium orthoferrite has been determined from full three-dimensional counter data and refined in the space group *Pbnm* by least squares to an accuracy of about 0·001 and 0·01 Å in positional parameters of Y^{3+} and O^{2-} respectively. Parameters are compared with those of $GdFeO_3$, derived by least-squares refinement of Geller's intensity data. It is found that the distortions from the ideal perovskite lattice hardly affect the octahedral environment of the Fe^{3+} ion, which makes it possible to predict Fe^{3+}–O^{2-}–Fe^{3+} angles in other distorted perovskite structures of known cell dimensions. Refinement in the alternative non-centrosymmetric space group $Pbn2_1$, shows small, possibly real, deviations from a centric structure.

Introduction

The magnetic properties of the orthoferrites having the chemical formula $RFeO_3$ (R = Y, La, Pr, Nd, Sm, Eu, Gd, Tb, Dy, Ho, Er, Tm, Yb and Lu) have been investigated at our Institute by a number of different techniques, such as magnetic measurements, Mössbauer spectroscopy and differential thermal analysis (Treves, 1962, 1964; Eibschütz, Gorodetsky, Shtrikman & Treves, 1964). In the course of these investigations the need was felt for information on the atomic parameters and especially on the variation of these parameters with varying R. The crystal structure of $GdFeO_3$ has been solved and refined by trial and error methods by Geller (1956), who also showed that all the members of the series are isostructural (Geller & Wood, 1956; see also Eibschütz, 1965). The crystal structure of $YFeO_3$ was chosen for an X-ray analysis because of

---

* The research reported in this article has been sponsored in part by the Air Force Materials Laboratory Research and Technology Division AFSC through the European Office of Aerospace Research, United States Air Force.

† This work was done in partial fulfilment of the Ph. D. requirements of one of the authors (M.E.).

the obvious advantage of Y being much lower in atomic number than other members of the series. At the same time we have found it useful to refine Geller's data on $GdFeO_3$ with the least-squares technique, which was not yet a standard method at the time of Geller's analysis.

Crystallographic constants and data collection

Crystals of $YFeO_3$ were kindly supplied by Mr J. P. Remeika of Bell Telephone Laboratories. A needle shaped crystal elongated along **c** and showing the forms {001} and {110} (orthorhombic symmetry) was cut with a razor blade to dimensions of 0·253 mm (||**c**) × 0·069 mm [$\perp(1\bar{1}0)$] × 0·054 mm [$\perp(110)$]. Data were collected on the G. E. Goniostat with nickel-filtered Cu *Kα* radiation. The intensity of a reflexion and the background in its vicinity were each counted for 10 seconds. Fluorescence of the Fe ion did not markedly increase the background since the volume of the crystal is very small. Absorption of radiation within the crystal, however, was very large and much attention had to be paid to a proper correction (see below).

Systematic absences were identical with those described by Geller: *h*0*l*, *h*+*l* odd; 0*kl*, *k* odd, being absent. Thus the space group is either *Pbnm* (D_{2h}^{16}) or *Pbn*2₁ (C_{2v}^{9}). Geller found that deviations from *Pbnm* are extremely small in $GdFeO_3$ and therefore this space group was used initially for the Y compound. At a later stage the structure was refined in the latter space group and small, possibly real, deviations from *Pbnm* were detected (see Table 3 and discussion below).

The cell dimensions were derived by a least-squares analysis of $\sin^2\theta/\lambda^2$ values of 30 high order reflexions. Results, given in Table 1, are in good agreement with cell dimensions determined from powder diagrams.

Table 1. *Cell dimensions of* $YFeO_3$ (Å)

	Present work 20°C	Geller (1958)	Eibschütz (1965)
a	5·2819 ± 0·0002*	5·280 ± 0·003	5·283 ± 0·003
b	5·5957 ± 0·0005	5·592 ± 0·003	5·592 ± 0·003
c	7·6046 ± 0·0004	7·602 ± 0·003	7·603 ± 0·003
D_x	5·696 g.cm^{-3}	5·71 g.cm^{-3}	5·70 g.cm^{-3}

* Based on least squares discrepancies, and do not include any effects caused by systematic errors.

Absorption correction

The absorption of X-rays in $YFeO_3$ is very large (μ = 879 cm^{-1} for Cu *Kα* radiation). Application of a recently developed method for absorption correction of diffraction intensities (Coppens, Leiserowitz & Rabinovich, 1965) made it possible to use data from a tiny crystal of non-spherical shape. This method uses vector algebra to calculate for every reflexion the absorption correction for each point of a Gaussian grid and has been programmed for our CDC 1604 computer. The over-all absorption correction is obtained as the weighted average over all the Gaussian grid points.

For $YFeO_3$ an exceptionally fine grid of 12 × 12 × 32 = 4608 points was chosen. As absorption generally exceeded 90% it was deemed necessary to check the absorption correction experimentally. This was done in two ways:

(*a*) Since the crystal was mounted with its *c* axis parallel to the *φ* axis of the Goniostat, it was possible to record 00*l* reflexions at various values of *φ* (by changing *φ* one merely rotates the crystal around the 00*l* scattering vectors). Absorption is however, dependent on *φ* as the crystal is not cylindrically symmetric. The absorption-corrected intensities showed little residual variation with *φ*, though before correction fluctuations up to 50% of the maximum value were observed.

(*b*) Both *hkl* and $h\bar{k}l$ reflexions were measured and corrected independently for absorption. Observed intensity differences between corresponding reflections were generally corrected satisfactorily by the procedure. A representative sample of reflexions is given in Table 2.

Table 2. *Comparison of some hkl and* $h\bar{k}l$ *reflexions before and after correction*

hkl	*I-B* (counts/sec)	Absorption factors*	F_{corr}
025	166	0·0463	78·0
$0\bar{2}5$	161	0·0463	76·8
125	24	0·0375	33·6
$1\bar{2}5$	30	0·0377	37·5
225	517	0·0613	127·3
$2\bar{2}5$	448	0·0541	126·2
325	39	0·0695	33·5
$3\bar{2}5$	34	0·0609	33·4
425	460	0·0802	98·0
$4\bar{2}5$	391	0·0696	97·0
525	190	0·0921	52·5
$5\bar{2}5$	167	0·0784	53·3
135	474	0·0444	145·0
$1\bar{3}5$	434	0·0432	140·7
235	2	0·0698	7·6
$2\bar{3}5$	2	0·0606	8·1
335	499	0·0810	106·4
$3\bar{3}5$	426	0·0691	106·5
435	139	0·0917	44·6
$4\bar{3}5$	126	0·0779	46·0
535	1451	0·1067	92·9
$5\bar{3}5$	1246	0·0912	93·1

* Defined as $A = I_{obs}/I_{corr}$.

The outcome of these checks gives confidence in the procedure employed and shows the feasibility of using specimens of arbitrary but well defined shape in the structure analysis of highly absorbing crystals.

The refinement

Refinement (on *F*) was carried out with a modified version of the Busing–Levy least-squares program on the CDC 1604 computer. A structure factor F_{hkl} was taken as the average of the absorption corrected values of F_{hkl} and $F_{h\bar{k}l}$. The standard deviation $\sigma(F)$ was derived in the usual way from $\sigma(I\text{–}B)$, which in turn

Table 3. *Final parameters of* $YFeO_3$

(x, y, z as fractions of unit-cell edges, B in Å^2)

		Without dispersion correction, centric	With dispersion correction, non-centric	With dispersion correction, centric	Undistorted perovskite
Y^{3+}	x	−0·0189 ± 0·0003	−0·0190 ± 0·0002	−0·0189 ± 0·0002	0
	y	0·0685 ± 0·0002	0·0679 ± 0·0002	0·0680 ± 0·0002	0
	z	0·25	0·25*	0·25	0·25
	B	0·06 ± 0·07	0·04 ± 0·05	0·09 ± 0·05	
Fe^{3+}	x	0	−0·0007 ± 0·0011	0	0
	y	0·5	0·5012 ± 0·0019	0·5	0·5
	z	0	0·0030 ± 0·0005	0	0
	B	0·29 ± 0·08	0·12 ± 0·06	0·26 ± 0·07	
O_I^{2-}	x	0·1089 ± 0·0002	0·1106 ± 0·0019	0·1109 ± 0·0019	0
	y	0·4632 ± 0·0021	0·4610 ± 0·0018	0·4614 ± 0·0019	0·5
	z	0·25	0·2510 ± 0·0034	0·25	0·25
	B	−0·15 ± 0·18	0·10 ± 0·15	0·21 ± 0·15	
O_{II}^{2-}	x	−0·3033 ± 0·0016	−0·3077 ± 0·0027	−0·3073 ± 0·0013	0·25
	y	0·3057 ± 0·0015	0·3048 ± 0·0028	0·3059 ± 0·0011	0·25
	z	0·0582 ± 0·0013	0·0520 ± 0·0024	0·0583 ± 0·0010	0
	B	0·14 ± 0·15	−0·63 ± 0·22	0·07 ± 0·11	
$O_{II}^{2-\prime}$	x		0·3075 ± 0·0033		
	y		−0·3066 ± 0·0038		
	z		−0·0677 ± 0·0028		
	B		0·43 ± 0·31		
R†		0·127	0·105	0·113	
R_w		0·0120	0·0060	0·0069	
$\{\Sigma\omega\Delta^2/(n-s)\}^{\frac{1}{2}}$		2·50	1·79	1·90	

* Not refined, defines origin in polar space group $Pbn2_1$.

$$\dagger\ R=\frac{\Sigma(|F_o-|F_c||)}{\Sigma F_o},\quad R_w=\frac{\Sigma\sqrt{w}(|F_o-|F_c||)}{\Sigma\sqrt{w}F_o},\quad \Delta=F_o-|F_c|,$$

n = number of observations included in refinement
s = number of parameters.

Table 4(*a*). *Observed and calculated structure factors of* $YFeO_3$

Reflexions marked * have been assigned zero weight, while the weights of those marked ** and *** have been reduced by a factor of 10 (** because of extinction, *** because of abnormal discrepancy between F_o and F_c).

h k ℓ	10 F_o	10|F_c|
2 0 0*	1120	1602
4 **	1007	1245
6	905	930
1 1 0***	302	213
2 ***	290	220
3	287	232
4	396	380
5	364	330
6	95	83
0 2 0*	900	1408
1	142	107
3	424	394
4	823	871
5	358	332
1 3 0	484	550
2	247	219
3	149	111
4	244	234
5	333	287
6	487	503
0 4 0	510	543
1	428	406
2	405	371
3	277	256
4	326	267
5	290	321
1 5 0	786	831
2	103	95
3	829	880
4	217	213
0 6 0	198	158
1	<36	36
2	320	291
3	264	247
1 7 0**	906	967
1 0 1	202	166
3	161	160
5	434	454
1 1 1	506	509
2	472	486
3	476	464
4	379	375
5	192	186
6	354	364
0 2 1***	498	678
1	190	150
2	755	825
3	159	148
4	591	605
5	313	312
6	414	381
1 3 1**	745	1076
2	118	109
3	688	713
4	198	187
5	566	549
6	33	42
0 4 1**	637	895
1	76	45
2	699	752
3	121	90
4	687	721
5	48	40
1 5 1	661	745
2	52	26
3	546	531
4	236	210
0 6 1	297	268
1	56	49
2	417	393
3	227	213
1 7 1	135	133
0 0 2	361	338
2	605	662
4	218	161
6	120	105
1 1 2*	1175	1627
2	291	241
3 *	1153	1553
4	<48	17
5 **	899	1015
6	295	287
0 2 2	426	476
1	352	338
2	154	114
3	259	235
4	115	83

Table 4(*a*) (*cont.*)

h k ℓ	10 F_o	10|F_c|
5	289	281
6	99	85
1 3 2**	674	871
2	65	61
3	631	636
4	399	389
5	672	678
6	357	393
0 4 2	516	613
1	<47	10
2	561	560
3	411	403
4	537	510
5	374	373
1 5 2	133	110
2	74	57
3	170	139
4	255	256
0 6 2	969	1012
1	212	190
2	826	854
3	141	140
1 0 3	393	367
3	337	326
5	466	483
1 1 3	608	616
2	245	311
3	198	151
4	424	442
5	402	376
6	294	300
0 2 3**	662	927
1	220	202
2	589	572
3	50	41
4	583	593
5	258	263
6	436	432
1 3 3**	759	921
2	290	271
3	740	791
4	45	20
5	459	436
0 4 3	488	566
1	113	83
2 **	791	902
3	78	67
4	659	665
5	53	32
1 5 3	655	654
2	184	163
3	556	543
4	40	32
0 6 3	447	426
1	142	139
2	279	259
3	175	163
0 0 4*	1244	1958
2 *	1127	1539
4 **	905	1067
6	736	782
1 1 4	229	188
2	76	42
3	328	301
4	147	161
5	299	269
6	172	176
0 2 4*	911	1350
1	121	110
2 **	991	1151
3	213	270
4	748	786
5	290	285
1 3 4	368	345
2	141	129
3	220	186
4	295	293
5	192	155
0 4 4	394	407
1	184	166
2	361	329
3	319	304
4	274	232
1 5 4	760	790
2	64	73
3	695	679
4	199	221
0 6 4	247	232
1	77	75
2	249	235

Table 4(*a*) (*cont.*)

h k l	10 F_o	10$\|F_c\|$	h k l	10 F_o	10$\|F_c\|$	h k l	10 F_o	10$\|F_c\|$
1 0 5	295	275	0 0 6	591	631	4 1 7	334	330
3	98	108	2	319	280	0 2 7	535	603
5	380	377	4	237	226	1	95	80
1 1 5	356	322	1 1 6**	1070	1193	2	501	487
2	368	352	2	<41	20	3	73	72
3	481	471	3 **	987	1075	4	469	474
4	296	284	5 **	815	898	1 3 7	705	713
5	104	86	0 2 6	133	111	2	170	152
0 2 5	422	469	1	66	31	3	614	612
1	194	165	2	190	180	0 4 7	534	537
2	691	715	3	266	260	1	59	50
3	182	177	4	99	71	2	660	685
4	532	512	5	246	270	0 0 8	1004	1037
5	289	291	1 3 6	571	557	2	1140	1174
1 3 5**	779	878	2	152	147	1 1 8	217	219
2	43	16	3	651	652	2	147	148
3	581	574	4	234	232	3	322	334
4	247	242	0 4 6	450	423	0 2 8**	909	1013
5	507	533	1 4 6	221	216	1	184	179
0 4 5**	719	872	2	497	455	2	719	703
1	<46	17	3	254	241	3	161	156
2	582	580	1 5 6	104	80	1 3 8	205	156
3	109	83	2	69	77	2	59	58
4	635	651	1 0 7	94	66	0 4 8	278	245
1 5 5	638	654	3	232	226	1 0 9	56	15
2	38	38	1 1 7	405	373	1 1 9	308	294
3	469	462	2	229	221	2	204	198
0 6 5	178	170	3	209	196	0 2 9	466	477
1	23	9						

was determined from the formula (Coppens & Schmidt, 1965):

$$\sigma^2(I-B)=\frac{I+B+2}{10}+c^2(I-B)^2$$

in which I is the observed intensity and B the background. The two terms on the right hand side of this expression allow respectively for the statistical error and an error, proportional to the intensity, resulting from slight missettings, extinction, errors in absorption correction, *etc.* The fit between absorption-corrected, symmetry-related intensities showed that the proportionality factor c should be about 0·03. During the course of this analysis Hartree–Fock–Slater scattering factor curves for Y^{3+} became available (Cromer, Larson & Waber, 1964), and these were used together with Fe^{3+} and O^{2-} scattering factor curves taken from *International Tables for X-ray Crystallography* (1962, p. 201) (in case of O^{2-} derived from f_O and f_{O^-}, *i.e.* $f_{O^{2-}}=2f_{O^-}-f_O$) and also based on self-consistent wave functions. The structure was refined both with and without corrections for anomalous dispersion. Values for the dispersive part of the scattering factor were taken from a compilation by Templeton (*International Tables for X-ray Crystallography*, 1962, p. 213); they are for Y, $f'=-0{\cdot}7$, $f''=2{\cdot}2$; for Fe, $f'=-1{\cdot}1$, $f''=3{\cdot}3$. Inclusion of these effects made remarkably little difference to the positional parameters (Table 3), though it did affect the scale and temperature factors and improved agreement between F_o and F_c. The $\mathrm{GdFeO_3}$ coordinates given by Geller were used as input parameters for the first least-squares cycle. 263 reflexions were included; seven of these were strongly affected by extinction and were given zero weight, while the weights of an additional seventeen reflexions which suffered from extinction to a lesser extent were reduced by a factor of 10. The same was done with the weights of three reflexions which showed abnormally large values of $w(F_o-F_c)^2$ after initial refinement.* All these reflexions are marked in the list of observed and calculated structure factors reproduced in Table 4(*a*). Five reflexions with $I-B$ smaller than $\sigma(I-B)$ were treated as unobserved: *i.e.* they are only included in the refinement when $|F_{\rm calc}|>\sigma(F)$. They could be all excluded on this criterion in the last of the seven cycles needed to obtain complete convergence. The same number of cycles was necessary for the refinement in space group $Pbn2_1$. No attempt was made to introduce anisotropic temperature factors, since all the thermal parameters are small and most of them do not differ significantly from zero. In a few cases negative thermal

Table 4(*b*). *Observed and calculated structure factors of* $\mathrm{GdFeO_3}$

Observed values are as reported by Geller (1956), but for difference in scale factor. Reflexions marked * have been assigned zero weight.

h k l	10 F_o	10$\|F_c\|$	h k l	10 F_o	10$\|F_c\|$	h k l	10 F_o	10$\|F_c\|$
1 1 0	891	985	4 4 5	1145	1160	2 1 7	313	347
2 2 0*	1360	2399	0 0 6	1116	1246	2 1 8	186	178
3 3 0	<215	93	1 1 6*	1478	1923	2 1 9	274	293
4 4 0	568	520	2 2 6	626	575	3 2 0	480	498
5 5 0	675	674	3 3 6	989	1017	3 2 1	333	343
1 1 1	773	823	4 4 6	509	430	3 2 2	372	385
2 2 1	1155	1309	1 1 7	675	572	3 2 3	137	136
3 3 1	1145	1284	2 2 7	871	890	3 2 4	382	383
4 4 1	1194	1277	3 3 7	1057	1085	3 2 5	343	365
5 5 1	910	818	4 4 7	1037	1013	3 2 6	392	361
0 0 2	1028	1240	0 0 8	1586	1739	3 2 7	196	194
1 1 2*	1507	2559	1 1 8	734	651	3 2 8	264	265
2 2 2	597	390	2 2 8	1184	1212	3 2 9	186	178
3 3 2	959	1134	3 3 8	<303	50	4 3 0	382	381
4 4 2	607	569	1 1 9	529	486	4 3 1	323	299
5 5 2	<333	30	2 2 9	891	776	4 3 2	519	639
1 1 3	803	883	0 0 10	1018	871	4 3 3	176	186
2 2 3	989	1105	1 1 10	1351	1420	4 3 4	440	497
3 3 3	1214	1408	1 0 3	352	303	4 3 5	362	296
4 4 3	1165	1176	1 0 5	401	352	4 3 6	411	372
5 5 3	920	919	1 0 7	<186	32	4 3 7	<196	187
0 0 4*	1781	2820	1 0 9	<196	43	4 3 8	421	519
1 1 4	871	830	2 1 0	<137	125	5 4 0	587	643
2 2 4*	1302	1786	2 1 1	480	624	5 4 1	<196	19
3 3 4	<343	28	2 1 2	392	273	5 4 2	587	614
4 4 4	489	432	2 1 3	470	497	5 4 3	<196	1
1 1 5	656	581	2 1 4	<157	112	5 4 4	499	593
2 2 5	1077	1093	2 1 5	470	447	5 4 5	<206	24
3 3 5	1096	1055	2 1 6	<215	28	5 4 6	460	557

Table 4(*b*) (*cont.*)

h k l	10 F_o	10$\|F_c\|$	h k l	10 F_o	10$\|F_c\|$	h k l	10 F_o	10$\|F_c\|$
1 2 0	127	79	2 3 1	264	224	3 4 3	<245	41
1 2 1	176	124	2 3 2	245	168	3 4 4	480	482
1 2 2	392	285	2 3 3	362	282	3 4 5	<264	119
1 2 3	313	338	2 3 4	313	248	3 4 6	372	397
1 2 4	147	167	2 3 5	166	147	3 4 7	<264	4
1 2 5	147	150	2 3 6	254	286	3 4 8	460	441
1 2 6	<166	96	2 3 7	254	179	4 5 0	460	563
1 2 7	176	126	2 3 8	186	132	4 5 1	264	220
1 2 8	186	164	2 3 9	186	151	4 5 2	411	386
1 2 9	196	105	3 4 0	460	456	4 5 3	<264	90
1 2 10	<186	70	3 4 1	<157	92	4 5 4	382	435
2 3 0	343	408	3 4 2	568	570	4 5 5	323	249
						4 5 6	382	463

---

* A factor of 10 was chosen in order to reduce ws^2 for these reflexions to values typical of the remainder of the data.

parameters were obtained (see Table 3 and also 5). They never differ significantly (*i.e.* more than three standard deviations) from zero and have obviously no physical meaning. It should be noted that the temperature factors obtained may be affected by incomplete allowance for extinction, uncertainties in the dispersive part of the scattering factor and the rather strong correlation between the scale and temperature factors.

Final parameters and agreement factors are listed in Table 3.

Refinement of $GdFeO_3$

Geller's Mo $K\alpha$ data on $GdFeO_3$, in which absorption effects were eliminated experimentally, were refined by the same least-squares procedure, using for Gd the recently published Hartree scattering factors (Cromer *et al.*, 1964) and allowing for dispersion effects (*International Tables for X-ray Crystallography*, 1962, p.213) (Gd, $f' = -0{\cdot}50, f'' = 4{\cdot}40$; Fe, $f' = 0{\cdot}30, f'' = 0{\cdot}90$).

Weights were taken to be proportional to $1/F^2$, which assumes $\sigma(F)$ to be proportional to F. Zero weights were assigned to the five reflexions most strongly affected by extinction (Geller, 1956). The weighted agreement factor dropped in seven cycles from 5·0% to 2·4%. The unweighted agreement decreased only slightly, because a number of extinction-affected, strong reflexions showed poor agreement between F_o and F_c and the weighting scheme successfully discriminated against these reflexions. Only the x parameter of O_I^{2-} and the z parameter of O_{II}^{2-} shifted significantly, the former by 0·3 Å (Table 5). As a result the parameters of O_I^{2-} are similar to those in $YFeO_3$ and the environment of the Fe^{3+} ion is almost octahedral. Values of F_o and F_c are listed in Table 4(*b*).

Table 5. *Parameters of* $GdFeO_3$

(x, y, z as fractions of unit-cell edges, B in Å^2)

		Geller (1956)	Our results, with dispersion correction
Gd^{3+}	x	−0·018	−0·0175 ± 0·0006
	y	0·060	0·0622 ± 0·0009
	z	0·25	0·25
	B		0·03 ± 0·13
Fe^{3+}	x	0	0
	y	0·5	0·5
	z	0	0
	B		−0·33 ± 0·23
O_I^{2-}	x	0·05	0·106 ± 0·009
	y	0·47	0·466 ± 0·007
	z	0·25	0·25
	B		0·4 ± 0·5
O_{II}^{2-}	x	−0·29	−0·296 ± 0·004
	y	0·275	0·275 ± 0·003
	z	0·05	0·062 ± 0·002
	B		0·0 ± 0·4
R		0·17*	0·15
R_w		0·050	0·024

* According to our calculations, slightly different from Geller's value because of different f curves (see text).

Discussion

The refinement of $YFeO_3$ in space group $Pbn2_1$ suggests two small deviations from the centric space group $Pbnm$ (Table 3). Firstly, the iron ion is shifted 0·0030 ± 0·0005 with respect to its position in $Pbnm$. Secondly, the oxygen ion O_{II}^{2-}, which is at x, y, z, and $\bar{x}, \bar{y}, \bar{z}$ in $Pbnm$, appears at x, y, z and $\bar{x}', \bar{y}', \bar{z}'$ in $Pbn2_1$, z and z' differing by slightly more than three standard deviations of their difference (taking into account the correlation coeficient −0·62 between z and z'). Both deviations are very small and it is not certain whether they are real. The following discussion is therefore based on the centric structure, the parameters of which are

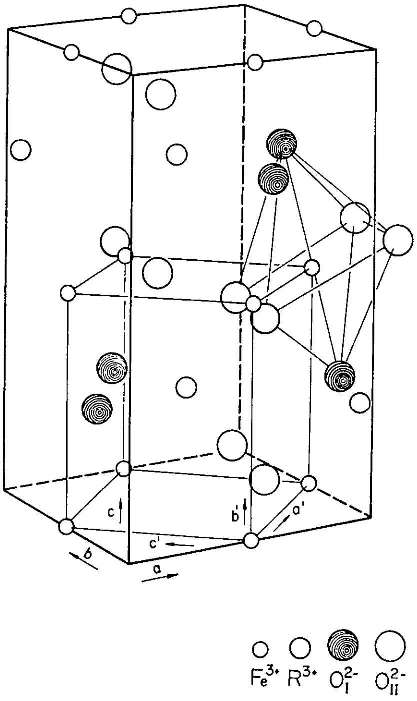

Fig. 1. The unit cell of orthoferrites $RFeO_3$. The monoclinic pseudocell is indicated by a', b' and c'. Notice the tilting of the octahedra around Fe^{3+}.

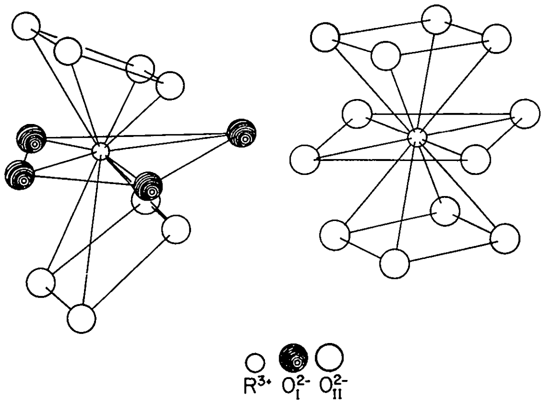

Fig. 2. The environment of the R^{3+} ion (*a*) observed for Y^{3+} and (*b*) in the undistorted perovskite lattice.

Table 6. *Distances* (Å) *in* $YFeO_3$ *and* $GdFeO_3$ (< 3·7 Å)

Ion		$YFeO_3$
Y^{3+}	4 O_I^{2-}	at 2·24±0·01; 2·31±0·01; 3·18±0·01; 3·46±0·01
	8 O_{II}^{2-}	at 2·263±0·007(2); 2·494±0·007(2); 2·691±0·007(2); 3·583±0·007(2)
	8 Fe^{3+}	at 3·077±0·001(2); 3·196±0·001(2); 3·357±0·001(2); 3·705±0·001(2)
Fe^{3+}	2 O_I^{2-}	at 2·001±0·003
	4 O_{II}^{2-}	at 2·003±0·007(2); 2·040±0·006(2)
	8 Y^{3+}	at 3·077±0·001(2); 3·196±0·001(2); 3·357±0·001(2); 3·705±0·001(2)
O_I^{2-}	10 O_{II}^{2-}	at 2·79±0·01(2); 2·81±0·01(2); 2·88±0·01(2); 2·90±0·01(2); 3·51±0·01(2)
	4 Y^{3+}	at 2·24±0·01; 2·31±0·01; 3·18±0·01; 3·46±0·01
	2 Fe^{3+}	at 2·001±0·003
	2 O_I^{2-}	at 3·16±0·01;
O_{II}^{2-}	6 O_{II}^{2-}	at 2·86±0·01(2); 2·86±0·01(2); 2·92±0·01; 3·11±0·01
	5 O_I^{2-}	at 2·79±0·01; 2·81±0·01; 2·88±0·01; 2·90±0·01; 3·51±0·01
	4 Y^{3+}	at 2·263±0·007; 2·494±0·007; 2·691±0·007; 3·583±0·007
	2 Fe^{3+}	at 2·003±0·007; 2·040±0·006
Ion		$GdFeO_3$
Gd^{3+}	4 O_I^{2-}	at 2·26±0·05; 2·36±0·04; 3·19±0·05; 3·41±0·04
	8 O_{II}^{2-}	at 2·38±0·02(2); 2·39±0·02(2); 2·82±0·02(2); 3·48±0·02(2)
	8 Fe^{3+}	at 3·119±0·004(2); 3·233±0·003(2); 3·384±0·003(2); 3·695±0·004(2)
Fe^{3+}	2 O_I^{2-}	at 2·01±0·01
	4 O_{II}^{2-}	at 2·08±0·02(2); 1·95±0·02(2)
	8 Gd^{3+}	at 3·119±0·004(2); 3·233±0·003(2); 3·384±0·003(2); 3·695±0·004(2)
O_I^{2-}	10 O_{II}^{2-}	at 2·80±0·04(2); 2·80±0·03(2); 2·98±0·03(2); 2·80±0·04(2); 3·66±0·05(2)
	4 Gd^{3+}	at 2·26±0·05; 2·36±0·04; 3·19±0·05; 3·41±0·04
	2 Fe^{3+}	at 2·01±0·01
	2 O_I^{2-}	at 3·20±0·06
O_{II}^{2-}	6 O_{II}^{2-}	at 2·85±0·03(2); 2·85±0·03(2); 2·88±0·02; 3·47±0·03
	5 O_I^{2-}	at 2·80±0·04; 2·80±0·03; 2·98±0·03; 2·80±0·04; 3·66±0·05
	4 Gd^{3+}	at 2·38±0·02; 2·39±0·02; 2·82±0·02; 3·48±0·02
	2 Fe^{3+}	at 2·08±0·02; 1·95±0·02

Table 7. Fe^{3+}–O^{2-}–R^{3+}, O^{2-}–R^{3+}–O^{2-} *and* O^{2-}–Fe^{3+}–O^{2-} *angles*

(*a*) Fe^{3+}–O_2^{-}–R^{3+} angles

	$YFeO_3$	$GdFeO_3$	Undistorted perovskite	Length of Fe^{3+}–O^{2-} and O^{2-}–Y^{3+}	Length of Fe^{3+}–O^{2-} and O^{2-}–Gd^{3+}
Fe^{3+}–O_I^{2-}–R^{3+}	104·7±0·3°	104·7±1·3°	90	2·00, 2·23 Å	2·01, 2·26 Å
	90·9±0·3	90·6±1·0	90	2·00, 2·31	2·01, 2·36
Fe^{3+}–O_{II}^{2-}–R^{3+}	79·8±0·2	79·3±0·7	90	2·04, 2·69	1·95, 2·82
	90·1±0·3	85·9±0·6	90	2·00, 2·69	2·08, 2·82
	85·6±0·3	88·1±0·7	90	2·00, 2·49	2·08, 2·39
	89·1±0·2	95·7±0·7	90	2·04, 2·49	1·95, 2·39
	96·9±0·3	92·6±0·7	90	2·00, 2·26	2·08, 2·38
	118·8±0·3	116·8±0·9	90	2·04, 2·26	1·95, 2·38

(*b*) O^{2-}–R^{3+}–O^{2-} angles

O^{2-}–R^{3+}–O^{2-} angles equal to 90° in undistorted perovskite:
$YFeO_3$ 118·1, 90·6, 63·1, 88·2, 71·6, 80·2, 81·7, 121·2, 102·9, 77·1°
$GdFeO_3$ 116·0, 91·5, 65·0, 87·5, 74·1, 74·5, 86·8, 116·0, 99·1, 83·2°

O^{2-}–R^{3+}–O^{2-} angles equal to 60° in undistorted perovskite:
$YFeO_3$ 73·8, 52·8, 51·9, 66·7, 70·8, 60·0, 58·7, 56·3, 48·1, 51·7, 70·7, 68·1°
$GdFeO_3$ 73·3, 54·4, 52·5, 65·7, 72·3, 58·1, 58·2, 54·4, 51·1, 53·3, 70·7, 64·6°

(*c*) O^{2-}–Fe^{3+}–O^{2-} angles

	$YFeO_3$	$GdFeO_3$	Undistorted perovskite
O_I^{2-}–Fe^{3+}–O_{II}^{2-}	88·2±0·2°	86·6±0·7°	90°
O_I^{2-}–Fe^{3+}–O_{II}^{2-}	88·3±0·2	90·0±0·7	90
O_{II}^{2-}–Fe^{3+}–O_{II}^{2-}	89·8±0·3	90·0±0·8	90

given in column 4 of Table 3 ($YFeO_3$) and column 3 of Table 5 ($GdFeO_3$) (see also Fig. 1).

The difference in sizes of the Y^{3+} and Gd^{3+} ions is reflected in the interatomic distances listed in Table 6; the shortest $Y^{3+}-Fe^{3+}$ distances, for example, are about 0·04 Å shorter than the corresponding $Gd^{3+}-Fe^{3+}$ distances. As Y^{3+} is the smaller ion, deviations from the ideal perovskite structure are larger in $YFeO_3$ than in $GdFeO_3$, as follows from comparison of the observed atomic parameters with those of the ideal perovskite structure listed in the last column of Table 3.

A detailed examination of the distortions shows that it is mainly the environment of R^{3+} that is distorted. The twelve $R^{3+}-O^{2-}$ distances, which are all equal in the undistorted perovskite lattice, vary largely in the present structures; similar variations are observed in $O^{2-}-R^{3+}-O^{2-}$ angles (Tables 6 and 7, and Fig. 2). The environment of the Fe^{3+} ion, on the other hand, is very nearly octahedral (Fig. 3). The $O^{2-}-Fe^{3+}-O^{2-}$ angles are 88·2 ± 0·2°, 88·3 ± 0·2° and 89·8 ± 0·3° in $YFeO_3$ and 86·6 ± 0·7°, 90·0 ± 0·7° and 90·0 ± 0·8° in $GdFeO_3$ (as compared with 83, 89 and 91° from Geller's (1956) $GdFeO_3$ parameters). There are small differences among the three $Fe^{3+}-O^{2-}$ distances (Table 6), but their average values are the same in both structures (2·01 Å) and very similar to those observed for the octahedrally coordinated iron atoms in yttrium-iron garnet (Geller & Gilleo, 1957) (2·00 Å) and gadolinium-iron garnet (Weidenborner, 1961) (2·00 Å).

This suggests that the average $Fe^{3+}-O^{2-}$ distance is independent of the distortion of the perovskite lattice, a conclusion not quite compatible with the theoretical interionic distances derived by Geller from the cell dimensions of orthoferrites (Geller & Wood, 1956; Geller, 1957) (respectively 1·914 and 1·930 in $YFeO_3$ and $GdFeO_3$ and 1·966 Å in the less distorted $LaFeO_3$). However, Geller's theory distributed distortions equally over the R^{3+} and Fe^{3+} environments, while our present results indicate that the main changes occur in the environment of R^{3+}.

Assuming the average $Fe^{3+}-O^{2-}$ distances to be 2·01 Å in all the orthoferrites we can calculate the angles $Fe^{3+}-O^{2-}-Fe^{3+}$, which are relevant to the superexchange interaction, with the formula $\sin\delta = l/4{\cdot}02$ in which δ is the angle FeOFe/2, l is either $c/2$ or $\frac{1}{2}\sqrt{a^2+b^2}$ and 4·02 is twice the average $Fe^{3+}-O^{2-}$ distance. The results, given in Table 8, are only meaningful as average values, and variations of ±0·04 Å in

Table 8. *Predicted and observed values of* $Fe^{3+}-O^{2-}-Fe^{3+}$ *angles in* $RFeO_3$ *compounds*

R	*a′*	$Fe^{3+}-O_{II}^{2-}-Fe^{3+}$ Predicted	$Fe^{3+}-O_{II}^{2-}-Fe^{3+}$ Observed	*b′*	$Fe^{3+}-O_{I}^{2-}-Fe^{3+}$ Predicted	$Fe^{3+}-O_{I}^{2-}-Fe^{3+}$ Observed
La	3·932 Å	156·0°		3·931 Å	155·8°	
Pr	3·912	153·4		3·905	152·5	
Nd	3·895	151·4		3·877	149·3	
Sm	3·885	150·2		3·856	147·2	
Eu	3·884	150·1		3·843	145·9	
Gd	3·877	149·4	148·3 ± 1·9°	3·834	145·0	145·3 ± 1·2°
Tb	3·865	148·1		3·818	143·5	
Dy	3·855	147·1		3·812	143·0	
Y	3·846	146·2	144·2 ± 0·6	3·802	142·1	143·6 ± 0·3
Ho	3·844	146·0		3·801	142·0	
Er	3·836	145·2		3·796	141·6	
Tm	3·830	144·6		3·792	141·2	
Yb	3·817	143·5		3·785	140·6	
Lu	3·806	142·4		3·783	140·4	

a′ and *b′* are dimensions of the monoclinic pseudocell (Fig. 1) taken from Geller & Wood (1956) and Eibschütz (1965)

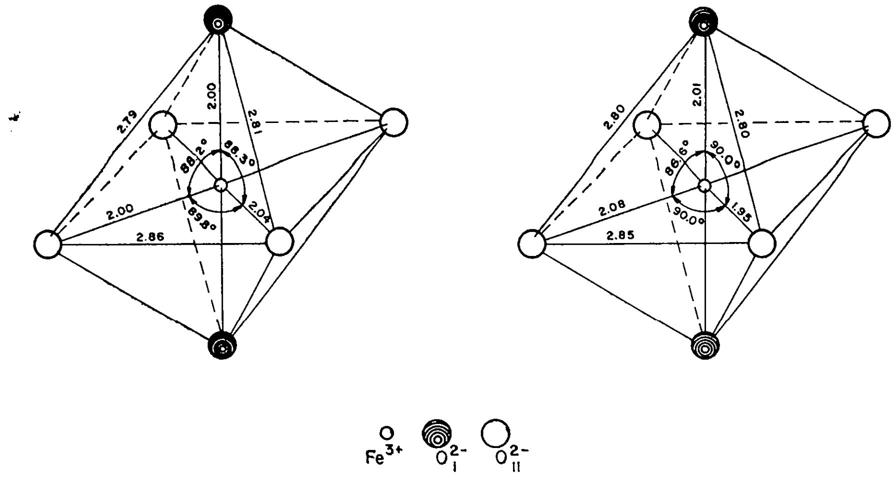

Fig. 3. The environment of the Fe^{3+} ion (*a*) in $YFeO_3$ and (*b*) in $GdFeO_3$

individual $Fe^{3+}-O^{2-}$ distances would cause deviations of almost 4° from the average $Fe^{3+}-O^{2-}-Fe^{3+}$ values.

One conclusion following from Table 8 is that even in $LaFeO_3$, which has an almost cubic unit cell, distortions from the ideal lattice are large, a conclusion reached earlier by Geller (1956) from examination of intensities of X-ray powder and single-crystal photographs.

Finally, the average deviation of the $Fe^{3+}-O^{2-}-R^{3+}$ angles from 90° is less than 9° in both structures, but one of these angles is increased to almost 120° (Table 7).

The authors would like to thank J. P. Remeika for preparing the single crystal and D. Treves for stimulating discussions.

References

Coppens, P., Leiserowitz, L. & Rabinovich, D. (1965). *Acta Cryst.* **18**, 1035.

Coppens, P. & Schmidt, G. M. J. (1965). *Acta Cryst.* **18**, 654.

Cromer, D. T., Larson, A. C. & Waber, J. T. (1964). *Acta Cryst.* **17**, 1044.

Eibschütz, M. (1965). *Acta Cryst.* **19**, 337.

Eibschütz, M., Gorodetsky, G., Shtrikman, S. & Treves, D. (1964). *J. Appl. Phys.* **35**, 1072S.

Geller, S. (1956). *J. Chem. Phys.* **24**, 1236.

Geller, S. (1957). *Acta Cryst.* **10**, 248.

Geller, S. (1958). *Acta Cryst.* **11**, 565.

Geller, S. & Gilleo, M. A. (1957). *Phys. Chem. Solids* **3**, 30.

Geller, S. & Wood, E. A. (1956). *Acta Cryst.* **9**, 563.

International Tables for X-ray Crystallography (1962). Vol. III. Birmingham: Kynoch Press.

Treves, D. (1962). *Phys. Rev.* **125**, 1843.

Treves, D. (1964). *Studies on Orthoferrites at the Weizmann Institute.* Presented at the 10th Annual Conference on Magnetism, Minneapolis.

Weidenborner, J. (1961). *Acta Cryst.* **14**, 1051.

Acta Cryst. (1965). **19**, 531

The Crystal Structure of Ammonium Sulfite Monohydrate

By Linda F. Battelle and K. N. Trueblood

Department of Chemistry, University of California, Los Angeles, California* 90024, *U.S.A.*

(*Received* 28 *January* 1965)

The structure of ammonium sulfite monohydrate has been determined in order to provide information about the geometry of the sulfite ion. It forms crystals of space group $P2_1/c$, with $a_0=6{\cdot}34$, $b_0=8{\cdot}08$, $c_0=12{\cdot}39$ Å, $\beta=97{\cdot}9°$, and four formula weights in the unit cell. The structure was readily solved by Patterson methods and was refined by full-matrix least squares; the hydrogen atoms were located in a difference map. Within experimental error, the sulfite ion is a trigonal pyramid, with the S–O distance 1·53 Å and the O–S–O angle 105°. The structure is held together by an efficient network of hydrogen bonds involving every hydrogen atom. This analysis provides another example of increasing bond distance with decreasing oxidation number in the oxyanions of third-row elements, observed earlier with the oxyanions of chlorine.

The geometrical and electronic structures of many of the oxyanions of third-row elements from Si to Cl, and of species related to these ions, have been investigated carefully in recent years (Cruickshank, 1961, 1964; Larson, 1965), but one notable lack has been the absence of any precise determination of the structure of the sulfite ion. The only previously reported structural study of the sulfite ion was that by Zachariasen & Buckley (1931), who determined the structure of anhydrous sodium sulfite. They reported the ion to be a trigonal pyramid, with the S–O distance 1·39 Å, the O–S–O angle 107°, and the sulfur atom displaced 0·51 Å from the plane of the three oxygens. However, their analysis was complicated by the apparent presence of twinning. Tang & Kuei (1956) considered further the nature of the twinning in this crystal, but did not give any structural information about the ion.

The S–O distance reported by Zachariasen & Buckley seems anomalously short, since it is about 0·10 Å shorter than that in the sulfate ion (Larson, 1965), whereas in the corresponding isoelectronic chlorine oxyanions, the Cl–O bond in chlorate ion (Laing & Trueblood, 1965) is about 0·04 Å longer than that in perchlorate (Cruickshank, 1961). It was for this reason that we undertook our study; we hoped at first to redetermine the structure of sodium sulfite, but difficulties with twinning made this impracticable. We therefore turned to $(NH_4)_2SO_3 . H_2O$, described by Groth (1908), after Marignac (1857).

Experimental

Initial attempts to obtain good single crystals of sodium, lithium, magnesium, and ammonium sulfites by recrystallization from aqueous solution failed because of air oxidation (to sulfate), twinning, or both. How-

---

* Contribution No. 1725.